Formation mechanism of single-wall carbon nanotubes on liquid-metal particles

Henning Kanzow* and Adalbert Ding
Technische Universität Berlin, Optisches Institut, Sekretariat P 1-1, Straße des 17. Juni 135, 10623 Berlin, Germany
(Received 9 April 1999; revised manuscript received 26 May 1999)

In this paper, we propose a mechanism for the formation of single-wall carbon nanotubes (SWCNT's) focusing on the possible transition state when tube formation is initiated. The model explains the generation of SWCNT's from carbon-metal plasmas as well as by the chemical vapor deposition technique. The model qualitatively predicts the experimentally observed dependences of the diameters of SWCNT's on the experimental parameters. It also explains why very high yields of SWCNT's can be achieved with mixed metal catalysts. [S0163-1829(99)02039-1]

I. INTRODUCTION

The formation of nanoscopic tubular carbon fibrils by the chemical vapor deposition (CVD) technique (decomposition of carbon containing gases like carbon monoxide or hydrocarbons on metal catalysts) was first reported in the 1950s.[1,2] The rapid improvement in the resolution of transmission electron microscopes made it possible to demonstrate that these fibrils are often multiwall carbon nanotubes (MWCNT's). Using controlled atmosphere electron microscopy, Baker performed detailed *in situ* studies of the growth of these fibrils and proposed a temperature driven diffusion mechanism for their formation.[3]

In the last decade, new methods for the production of bundles of single-wall carbon nanotubes (SWCNT's) have been developed which are based on the covaporization of pure carbon and a metal catalyst either in an electric arc discharge[4–10] or by high power laser irradiation.[11–13] The models proposed for the formation usually start from the carbon-metal gas phase. Open fullerene structures in the shape of half bowls are formed first. Metal clusters or atoms hinder the closure of the bowls and further carbon atoms or units are incorporated, leading to tube growth.[14,15] Unfortunately there is still little experimental support for these gas phase theories, simply because direct studies are very difficult to undertake. These theories also do not predict the change of the properties of the tubes as a function of the experimental parameters used.

However, in the last few years, SWCNT's have also been generated with CVD techniques.[16–19] The formation of the SWCNT's by CVD certainly cannot be explained by a homogeneous gas-phase reaction. The low temperatures of usually 1000 to 1200 °C in the CVD experiments do not allow for the evaporation of the metal catalysts. Recently, Hafner *et al.* reported the generation of SWCNT's by the catalytic decomposition of carbon monoxide and ethylene over alumina supported molybdenum and iron-molybdenum catalysts at temperatures between 700 and 850 °C. It was demonstrated that at these low temperatures SWCNT rather than MWCNT growth occurred, when the carbon supply was stricly limited to an unusual low level.[18]

In a CVD-type reaction we produced chains of multiwall carbon nanoparticles from fullerenes.[20] Chains of hollow multiwall particles are also known to be a product of electric carbon-metal arc discharge.[6,7] This inspired us to take a closer look at the similarities of the different production methods of SWCNT's.

II. CHEMICAL VAPOR DEPOSITION

The diffusion model is well established for the growth of MWCNT's from carbon containing gases.[21] The idea originates from the vapor-liquid-solid mechanism (VLS) for the formation of whiskers.[22] In this theory gaseous compounds are decomposed effectively on the surface of catalytic metal droplet. The resulting supersaturated liquid precipitates the solute continuously in the form of faceted cylinders.

The most time consuming step for the formation of MWCNT's on metal particles is the diffusion of the solute from the decomposition site to the segregation site. This explains why Baker *et al.*[3] found a remarkable correlation between the activation energies directly measured for the growth of the carbon fibrils and those for the diffusion of carbon through the corresponding metals. A diffusion mechanism is also strongly supported by an experiment with a nickel tube:[23] Methane was passed through the tube for one hour in a hot argon atmosphere ($T = 1000\,^{\circ}\mathrm{C}$). Electron microscopy showed that after the reaction the inside surface, which had been exposed to the hydrocarbon, was coverd with black amorphous carbon resembling soot, while the deposit on the outer surface was a gray multi-wall graphitic skin.

With simple thermodynamic equations, Tibbetts has shown that carbon originated from natural gas and precipitated from small particles forms MWCNT's with inner diameters larger than 5 nm.[24] The tube outer diameter is determined by the particle size of the catalyst. The diffusion model also explains why the growth of MWCNT's favors a certain metal cluster size of 2 to 100 nm:[21] If the catalytic particle is too large, the diffusion length for the carbon is too long. If the particle is too small, the strain energy of the graphitic tube with an appropriate diameter is too great. However, Tibbetts model is too static to describe the formation of SWCNT's (not known at that time).

There is no agreement in the literature about whether the carbides of the iron group take part in the formation of MWCNT's. Cementide (Fe_3C) and other iron carbides are frequently observed after the reaction of hydrocarbon or car-

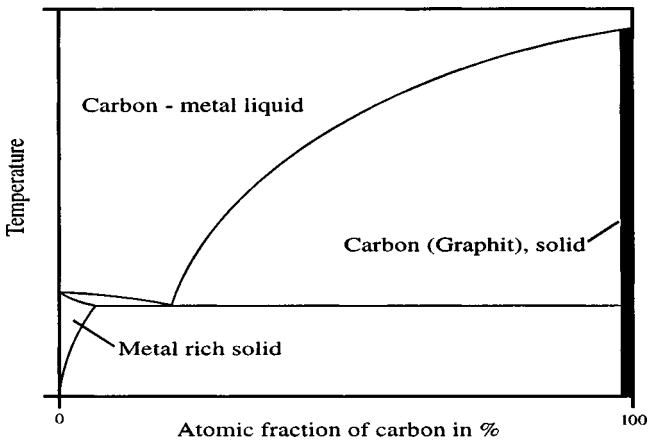

FIG. 1. Schematic carbon-metal phase diagram.

bon monoxide with iron catalysts.[25–27] The activities of iron catalysts seem to correlate with their carbide content.[26] Pure cementite, however, does not promote the generation of nanofibers.[28] The observed kinetics of the fiber growth also rather support the idea of a diffusion through pure metals.[3] So the observed increased activity of cementide containing iron catalysts may be a result of the surface breakup of the metal.[26] But the situation becomes even more complicated because oxygen is usually also present during the reaction. The oxygen originates from the support material or is part or contaminant of the gaseous feedstock (e.g., carbon monoxide, aceton in methane or acetylene). Oxygen can produce wüstite (FeO),which is a very active catalyst for the formation of nanofibers.[28] A formation mechanism concerning both the cementide as well the wüstide was proposed by Stewart *et al.*[29] An increase of the activity of cobalt catalysts by oxygen was observed by A. Fonseca *et al.* They speculate that the oxygen might have a positive effect on the surface properties of the metal particles and hinders their agglomeration.[30]

We believe that the concept of diffusion through the particle is basically correct for all kinds of carbon nanotube growth. But in order to explain SWCNT's we find it is important to concentrate more on the beginning of the tube formation, an area also treated by H. Dai *et al.*[16]

III. CARBON-METAL PLASMA EXPERIMENTS

Before presenting the SWCNT formation mechanism we want to concentrate on the complex processes that occur outside the carbon-metal plasma by which SWCNT's have been frequently generated: A first approximation is given by the phase diagrams. The binary alloy diagrams of carbon with the standard single-metal catalysts (nickel or cobalt) consist of simple eutectics, with a very limited solubility of the metals in the graphitic carbon phase. The high temperature ($T > 1153\,^{\circ}\mathrm{C}$) carbon rich part of the iron-carbon phase diagram shows similar characteristics.

Considering the schematic diagram (Fig. 1) we expect carbon-metal vapors to condense as liquids after leaving the hot plasma. When a carbon rich melt is further cooled, a metal-free carbon phase will be segregated. Finally, when the eutectic point is reached, a metal-rich phase and more carbon is deposited on these carbon particles. These metal coated carbon particles float in the gas phase of the reactor. In the arc discharge system many are attracted by the electric field and form a deposit on the hot cathode. If these metal rich particles on their carbon substrate are in a hot environment, they can react with the gaseous compounds like stable and unstable fullerenes or small amorphous carbon particles in a CVD way. Fullerenes are a typical by product of carbon-metal plasmas. Smoke particles were directly caught on TEM grids at different distances from a carbon-metal plasma by Saito *et al.*[9] Their investigation showed that small metal particles were indeed formed first in the gas phase and then SWCNT's grew from them.

At lower temperatures the situation is much more complicated, as the metal-carbon mixtures are solid and can form various phases. Though carbides of these iron group metals are not thermodynamical stable,[31,32] especially iron tends to form metastable carbide phases. Therefore carbide particles as well as pure metal particles are generated in the arc discharge method when the graphitic electrodes are doped with iron group metals.[6] Their spherical nature indicates that they were in the liquid state before rapidly cooling down. It should also be noted that other metals like molybdenum form stable carbides at moderate temperatures. In these cases, the carbides are certainly a central factor for the understanding of the formation of nanofibers.

To avoid all complications and effects which are related to carbides and oxides we restrict our following considerations to the more simple carbon-metal systems at higher temperatures in the absence of any oxygen contamination.

IV. MODEL

The products of the plasma methods and the CVD technique are identical, therefore it is reasonable to assume that the formation processes are the same. This assumption is supported by another observation: The metal particles found in the product of the plasma experiments[6,7,11] have the same sizes found to be active for the fiber formation in the CVD experiments.[19,24] Also important for the understanding of our model is the following: High-resolution TEM pictures of bundles of SWCNT's show that the size distribution of the tube diameters within the bundles is very narrow.[7,11,12] This implies that they have experienced similar growth conditions. Therefore, it is likely that they grew at the same catalytic site. The details of the growth model are presented in Fig. 2.

(1) As explained earlier the starting point for the fiber growth is most likely a small metal rich particle in contact with a substrate. In the plasma methods the substrate is a carbon particle either floating in the gas phase or attached to the cathode in the case of the plasma arc method.

If the catalytic particle is big enough[24] and the carbon supply is high[18] or there is not enough energy in the system (explained later), multiwalled growth takes place. Multiwall growth is usually obeserved at low temperatures ($T < 900\,^{\circ}\mathrm{C}$), at which the metal does not melt and therefore cannot change its shape. This situation is shown in the left reaction path in Fig. 2.

(2) Carbon containing gas molecules (e.g., hydrocarbons, fullerenes) are exothermally decomposed on the surface of the particle, resulting in the heating of this surface. The car-

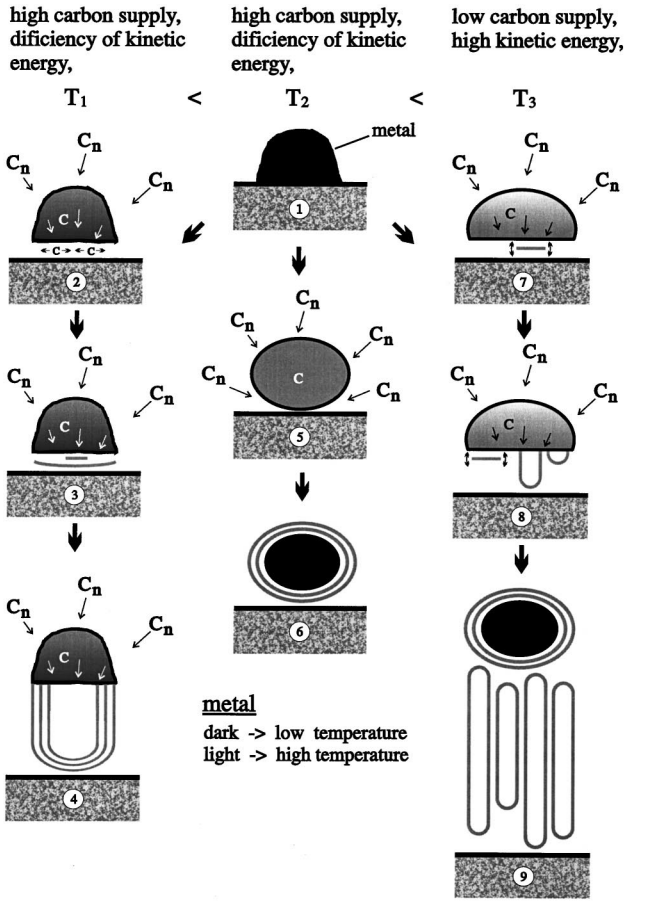

FIG. 2. Growth model for carbon nanostructures from the reaction of carbon containing gases with metal-rich particles on a carbon substrate at different temperatures and carbon supply conditions.

bon is absorbed and diffuses towards the cooler region of the metal near the substrate. For thermodynamic reasons less carbon can be dissolved in this cooler region than in the hot area on the upper surface.[31] The supersaturation on the cooler side leads to the segregation of carbon atoms. They move on the surface to combine and form a first graphitic layer. If there is not enough kinetic energy in the system, this layer will not bend to form a small cap (7),(8) and continue to grow. Even if there is enough kinetic energy, it is very unlikely that the layer, which is too big, will bend. The bending of the graphitic sheet (7),(8) requires a coordinated movement of the carbon atoms away from the particle surface. For statistical reasons this movement is very unlikely if the sheet contains too many atoms. So in the case that the carbon supply is high, the graphitic layer will rapidly grow over the limit of statistical favorability.

(3) More graphitic planes are generated, causing the previous planes to bend. The bending of the graphitic planes stabilizes the unsaturated sp^2 orbitals at the border of the graphene sheets by overlapping with the orbitals of the metal.

(4) This contact then serves as a crystallization seed for the following segregation of carbon. A cylindrical multiwall growth is initiated.

It should be mentioned that we may have oversimplified the growth of MWCNT's on a solid catalyst as the crystal orientation may also be of importance in the growth process. Therefore, bidirectional growth can be observed in CVD experiments.[33]

At medium temperatures the metal is melted and the crystal orientation is lost. This situation is shown in the middle reaction path in Fig. 2.

(5) The exothermic nature of the decomposition of carbon compounds, the lowered melting point because of the absorbed carbon, and the high-surface energy cause the metal rich particles to melt at medium temperatures. Because of its surface energy a droplet loses contact with the substrate and the carbon containing gases can attack from all directions. No cooler region exists for the initiation of fiber growth.

In our own experiments we observed that the temperature for this process for small nickel particles is around 1000 °C in an argon atmosphere.[20] However, the contact angle of a metal is strongly dependent on the surface and adhesion energy between the metal and the substrate, which are in turn dependent on the gas composition.[34] This means the temperature range can shift significantly. In CVD experiments hydrogen often is an important component in the gas composition. A hydrogen atmosphere in general leads to a much better wetting behavior, the contact angle of the metal on the carbon substrate is strongly affected. Another way to avoid melting and loss of contact is to use a metal with a high melting point.

(6) The high degree of supersaturation will eventually cause spontaneous precipitation of carbon on all over the surface of the metal-rich droplet. Encapsulated nanoparticles result. Alternatively the reason for not forming any small caps and in this way SWCNT's like in (7),(8) may be again due to the too fast growth of the graphitic sheet or the deficiency of kinetic energy.

At higher temperatures the contact angles of metal droplets on graphite decrease,[35] which will again increase the contact area. The situation in the high-temperature range is shown in the right reaction path in Fig. 2.

(7) At high temperatures the carbon is absorbed and precipitated as in (2). But if the system contains enough kinetic energy, the graphitic plane is able to oscillate in respect to the metal surface in such a way that a small cap is formed. This cap formation is also assisted by the fact that bonds fluctuate at such temperatures and the atoms are able to change their positions to form five membered rings. The crucial step of the plane oscillation allows us to make qualitative predictions about the average tube diameter. This will be discussed later in more detail.

It is not clear if it is correct to also use the supply argument for this high-temperature region. The experiments on which this argument is based were done at lower temperatures with catalytic metals which tend to form solid carbide phases in that temperature range.[31] Nevertheless, the idea fits well in this model that a too rapid growth of the graphitic sheet would also sharply reduce the statistical probability of bending the sheet into a cap.

(8) The bending of the graphitic plane stabilizes the unsaturated sp^2 orbitals on the border of the graphene sheets because of the overlap with the metal orbitals. The contact then serves as a crystallization seed for the subsequent segregation of carbon. A single-wall growth is initiated. The strong binding forces between the border of the cap and the

metal and the tubular growth hinders the bent graphitic plane from further oscillation. The processes (7) and (8) will also occur on neighboring positions on the same particle. Because the reaction conditions are similar, the diameters of the tubes will be similar. A rope of SWCNT's with nearly identical diameters starts to grow.

An alternative explanation for generating ropes is given by P. Bernier:[36] He observed frequently that the tubes of a bundle often do not end at the same place and concluded that the tubes grow individually and align later. This coagulation idea might be also important to explain why multidirectional growth of bundles of SWCNT's on one metal particle can be observed.[8] It is likely that metal droplets attached to bundles of SWCNT's coagulate, forming a larger metal particle with several associated bundles.

(9) The melt solidifies when the temperature drops below the eutectic temperature of the system. Because much more carbon can be dissolved in a melt than in a solid,[31] the extra carbon stored in the particle is segregated at once. This closes the tips of the tubes and encapsulates the metal droplet.

V. DISCUSSION

In this section, we focus on the energetics of the crucial step for the growth of SWCNT's, which is the oscillation of the graphitic plane shown as (7) in Fig. 2. It allows us to qualitatively predict the experimentally observed dependences of the diameters of SWCNT's on the experimental parameters.

We believe that a certain angle—we will call it the minimum overlap angle—of the unsaturated sp^2 orbitals on the edges of the graphitic plane must be reached to obtain a significant stabilizing interaction with the metal orbitals. Otherwise the plane will flatten out again and the graphitic cap will not be stable for the amount of time needed to initiate tube growth. After the border of the cap has formed strong bonds to the metal and especially when a short tube has been formed, flattening out would require a huge amount of energy, which is not available.

There are two forces that have to be overcome in order to bend the plane: The surface tension of the sheet and the work of adhesion between the graphitic sheet and the metal. The kinetic energy in the system available for bending the plane is proportional to temperature T and the size of the sheet. The upper temperature limit for growth of SWCNT's is approximately 2000 °C. At higher temperatures SWCNT's are destroyed.[37] For avoiding complications with solid metal phases (e.g., cementide) we arbitrarily set the lower temperature limit to 1000 °C.

Because very high yields of SWCNT's can be reached with optimized reaction parameters,[10,11] the processes for the tube formation must be very efficient. This means that the effective average kinetic energy E_{kin} stored per carbon atom on the carbon-metal interface in one degree of freedom must be greater than the work of adhesion per carbon atom W_{Ad} in the graphitic sheet:

$$E_{kin} - W_{Ad} > 0. \tag{1}$$

As atoms from both sides of the interface contribute to the kinetic energy available for bending the graphitic plane, the effective energy for one carbon atom E_{kin} in the graphitic sheet is approximately

$$E_{kin} \approx \frac{(0.5 \cdot k \cdot T)}{A_C} + \frac{(0.5 \cdot k \cdot T)}{A_{CM}}, \tag{2}$$

where T is the temperature in K and k the Boltzmann constant. The area occupied by one carbon atom in a graphitic sheet A_C was calculated from the interatomic distance ($d_{C-C} = 1.42 \cdot 10^{-10}\ m$) to be

$$A_C = 2.44 \cdot 10^{-20}\ m^2. \tag{3}$$

Assuming a cubic face-centered structure, we estimated the area occupied by one atom on the surface A_{CM} of the melt to be

$$A_{CM} = [X_C \cdot d_{C-C} + (1 - X_C) \cdot d_{M-M}]^2. \tag{4}$$

X_C is the atomic fraction of carbon in the melt and d_{M-M} the interatomic distance of two metal atoms, which is approximately $2{,}32 \cdot 10^{-10}\ m$ for either cobalt, iron, or nickel. The work of bending, W_B, needed to overcome the surface tension rises with the degree of bending of the graphitic sheet. If only a little more kinetic than adhesion energy per atom is available in the system, a large graphitic sheet has to grow until the minimum overlap angle can be reached with a larger cap diameter. If the energy difference is large and positive, the minimum overlap angle can also be reached with a smaller sheet and tubes with smaller diameters will be formed.

In the following, we want to examine how the average diameter of SWCNT's qualitatively change in our model, if we change the catalytic metal or the formation temperature. First some of the experimental results from other groups.

1. Recently Guo *et al.* reported that the average diameters of the SWCNT's produced by laser ablation of metal-graphite composites increase with higher ambient temperatures.[13]

2. Seraphin shows histograms of the diameters of SWCNT's produced in a carbon-metal arc with either cobalt, iron, or nickel.[7] She found that in the iron and nickel samples most tubes were in the similar range of 0.70 to 1.00 nm, while in the cobalt sample the average nanotube diameters were larger and the distribution broader; most tubes had diameters varying between 0.85 and 1.30 nm. When using mixed metal catalyst the yield of SWCNT's increased sharply. This was accompanied with large average diameters and especially broad diameter distributions. Similar results for the diameter distributions with the different metal catalysts were also reported by Saito *et al.*[9]

Data to the diameter dependences on the temperature and the different metal catalysts in CVD experiments at high temperatures are not available so far.

To estimate the maximum energy available for bending the planes we must know the adhesion energies W_{Ad}. We postulate that the adhesion energy of a metal-carbon droplet towards graphite can be expressed as a simple linear addition of the adhesion energies of the pure components carbon ($W_{Ad,G}$) and metal ($W_{Ad,M}$) towards graphite according to their atomic fraction X

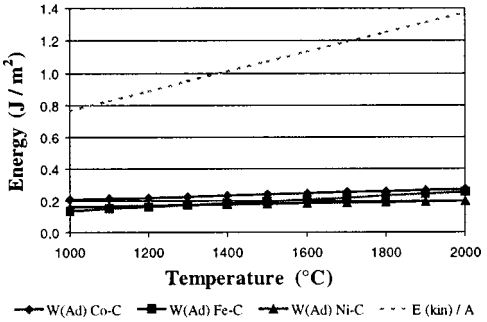

FIG. 3. Comparison of the kinetic and adhesion energies per area of an atomic carbon fraction of $X_C = 0.95$ in the metal-carbon droplet related to the bending process shown in Fig. 2 (7).

$$W_{Ad} = (1 - X_C) \cdot W_{Ad,M} + X_C \cdot W_{Ad,G}\,. \tag{5}$$

One should have in mind that this is only a rough approximation of the real surface concentrations. It is known that certain elements are enriched on the surfaces of metal droplets.[34] This enrichment will also be strongly temperature dependent.

The temperature dependence of the adhesion energies of the pure metals $W_{Ad,M}$ cobalt, nickel or iron towards graphite was estimated from the data of Weisweiler and Mahadevan[35] by a linear inter- and extrapolation of the two or three data points measured. This is a legitimate procedure as most thermodynamic surface properties have a wide linear temperature range. Data of the surface energy of liquid carbon was not available. Therefore, we used the adhesion energy of a graphitic plane on graphite, which is two times the surface free energy of graphite $E_{S,G}$. In this way, we may slightly overestimate the real value for the adhesion energy of a graphitic plane on liquid graphite

$$W_{Ad,G} = 2 \cdot E_{S,G}\,. \tag{6}$$

The temperature function of the surface free energy of graphite $E_{S,G}$ was obtained by a linear fit of the values given by Abrahamson[38] excluding the 0-K value.

We tried to calculate the temperature function of the atomic fraction of cobalt, iron, and nickel in a carbon-metal droplet in equilibrium with fullerene C_{60} vapor at temperatures between 1000 and 2000 °C. Because of the large amount of free energy stored in C_{60} (Ref. 39) there is no equilibrium condition state at the reasonable pressures of 10^{-5} to 1 bar C_{60}. Fullerenes will therefore not stop being adsorbed by the droplet even if the carbon atomic fractions X_C are very close to 1. This means that the value for X_C is only dependent on the kinetics of the absorption and precipitation reactions. As we have not calculated the kinetics, we can only estimate X_C to be greater than the (temperature dependent) equilibrium value for X_C of a carbon-metal droplet in contact with graphite. However, the carbon fraction must be lower than the composition originally evaporated, since the polycrystalline graphitic carbon segregated above the temperature limit of approximately 2000 °C will most probably be partly inactive for the transformation into tubes.[20] During the growth of the tubes a further enrichment of metal takes place: While carbon is transformed into tubes the metal accumulates, if it does not encapsulated or leave the hot reaction region.

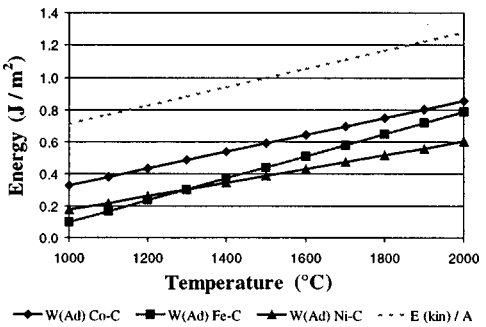

FIG. 4. Comparison of the kinetic and adhesion energies per area of an atomic carbon fraction of $X_C = 0.83$ in the metal-carbon droplet related to the bending process shown in Fig. 2 (7).

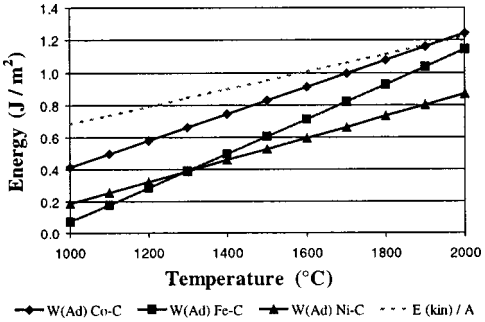

FIG. 5. Comparison of the kinetic and adhesion energies per area of an atomic carbon fraction of $X_C = 0.75$ in the metal-carbon droplet related to the bending process shown in Fig. 2 (7).

Figures 3–6 show the temperature dependence of the adhesion and kinetic energies per surface area of one carbon atom in the graphitic sheet for the metals cobalt, iron and nickel of different atomic fractions X_C of the carbon in the liquid carbon-metal droplet calculated after the Eqs. (1)–(6).

Figure 3 demonstrates that for high-carbon fractions the differences in the adhesion energies of the different melts towards graphite are small compared with the part of the kinetic energy available for bending the tubes. This means that the diameters of the tubes would not vary significantly if the catalytic metal is changed. Also we predict that the diameters of the tubes would slightly increase with the reaction temperature. This system of high-carbon content does not show the characteristics we expected from the experiments mentioned earlier.

For the atomic fraction of approximately 0.83 (Fig. 4) the difference between the metals becomes more apparent: For

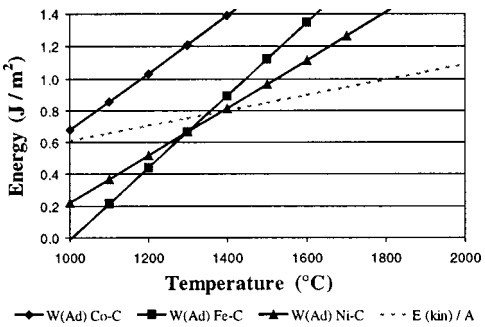

FIG. 6. Comparison of the kinetic and adhesion energies per area of an atomic carbon fraction of $X_C = 0.50$ in the metal-carbon droplet related to the bending process shown in Fig. 2 (7).

the lower temperature range below 1500 °C, the growth of nanotubes with larger diameters is expected for cobalt. The higher amount of kinetic energy will yield smaller diameters when nickel or iron is used as a catalyst, as was experimentally observed.[7,9] The diameters are almost independent of the temperature that is not in accordance with the work of Rao *et al.*[13]

For the carbon atomic fraction from approximately 0.70 to 0.80 (Fig. 5), the difference between cobalt on the one side and nickel and iron on the other side remains the same: Tubes with larger diameters are expected for cobalt, while smaller diameters are expected for nickel or iron as catalyst as observed by Seraphin,[7] and Saito, Koyama, and Kawabata.[9] The diameters increase with temperature for all the metals we calculated, because the decreased amount of kinetic energy will result in larger diameters. This is in good accordance with the results of Rao *et al.*[13]

The higher the metal content in the catalytic droplet, the greater is the adhesion energy towards graphite. Therfore, our model also predicts larger diameters of SWCNT's if a larger amount of the metal is evaporated in the plasma experiments. It would be very interesting to do this experiment. If the metal contents are very high, the kinetic energy may not be sufficient to compete with the higher adhesion energies. In Fig. 6 it is demonstrated that there is no temperature above 1000 °C at which SWCNT's can be formed if the atomic fraction for cobalt is higher than approximately 0.50. So no tubes are formed if too much metal is used in the plasma methods.

A last remark is dedicated to describing the relative yields of nanotubes with different metal catalysts: Comparing the yields of SWCNT's in the carbon-metal arc experiments, it is obvious that cobalt is a much better catalyst than nickel or iron.[5,7,9] In Fig. 2, we have shown that the contact between the substrate (amorphous or polycrystalline carbon) and the catalytic droplet is very important. Cobalt has a better contact over a much wider temperature range below 2000 °C. This means that growth can be initiated at a larger surface area at greatly varying temperatures resulting in a widening of the tube diameter distribution. This is also in accordance with the data from Seraphin.[7] By mixing metals it is possible to dramatically increase the yields.[7,9–11] Good catalyst like cobalt:nickel=1:1 and cobalt:iron=1:1 result in a very broad diameter distribution, indicating very different reaction temperatures in accordance with our model.

VI. CONCLUSION

We have proposed a model for SWCNT's formation on metal particles focusing on the free-energy situation of the possible transition state when tube growth is initiated. The model predictions about the dependence of SWCNT's diameter on the reaction parameters are in good qualitative agreement with the observations from other groups. It also explains the high yields, which can be achieved with mixed metal catalysts.

ACKNOWLEDGMENTS

This work has been funded by the German Ministry of Science and Technology (BMBF) under Contract No. 13N6705 and from the SFB 337.

*FAX:++49/30/3 14-27 85 0. Electronic address: kanzow@physik.tu-berlin.de

[1] L.V. Radushkevich and V.M. Lukyanovich, Zh. Fiz. Khim. **26**, 88 (1952); **47**, 6210 (1953).
[2] L.J.E. Hofer, E. Sterling, and J.T. McCartney, J. Phys. Chem. **59**, 1153 (1955).
[3] R.T.K. Baker, M.A. Barber, P.S. Barber, P.S. Harris, F.S. Feates, and R.J. Waite, J. Catal. **26**, 51 (1972).
[4] S. Iijima and T. Ichihashi, Nature (London) **363**, 603 (1993).
[5] D.S. Bethume, C.H. Kiang, M.S. de Vries, G. Gorman, R. Savoy, J. Vazquez, and R. Beyers, Nature (London) **363**, 605 (1993).
[6] Y. Saito, T. Yoshikawa, M. Okuda, N. Fujimoto, K. Sumiyama, K. Suzuki, A. Kasuya, and Y. Nishina, J. Phys. Chem. Solids **54**, 1849 (1993).
[7] S. Seraphin, J. Electrochem. Soc. **142**, 290 (1995).
[8] Y. Saito, M. Okuda, M. Tomita, and T. Hayashi, Chem. Phys. Lett. **236**, 419 (1995).
[9] Y. Saito, T. Koyama, and K. Kawabata, Z. Phys. D **40**, 421 (1997).
[10] C. Journet, W.K. Maser, P. Bernier, A. Loiseau, M. Lamy de la Chapelle, S. Lefrant, P. Deniard, R. Lee, and J.E. Fischer, Nature (London) **388**, 756 (1997).
[11] T. Guo, P. Nikolaev, A. Thess, D.T. Colbert, and R.E. Smalley, Chem. Phys. Lett. **243**, 49 (1995).
[12] W.K. Maser, E. Muoz, A.M. Benito, M.T. Martnez, G.F. de la Fuente, Y. Maniette, E. Anglaret, and J.-L. Sauvajol, Chem. Phys. Lett. **292**, 587 (198).
[13] A.M. Rao, S. Bandow, E. Richter, and P.C. Eklund, Thin Solid Films **331**, 141 (1998).
[14] Y.H. Lee, S.G. Kim, and D. Tomnek, Phys. Rev. Lett. **78**, 2393 (1997).
[15] A. Maiti, C. Brabec, C. Roland, and J. Bernholc, Phys. Rev. B **52**, 14 850 (1995).
[16] H. Dai, A.G. Rinzler, P. Nikolaev, A. Thess, D.T. Colbert, and R.E. Smalley, Chem. Phys. Lett. **260**, 471 (1996).
[17] A. Peigney, C. Laurent, F. Dobigeon, and A. Rousset, J. Mater. Res. **12**, 613 (1997).
[18] J.H. Hafner, M.J. Bronikowski, B.R. Azamiam, P. Nikolaev, A.G. Rinzler, D.T. Colbert, and R.E. Smalley, Chem. Phys. Lett. **296**, 195 (1998).
[19] H.M. Cheng, F. Li, G. Su, H.Y. Pan, L.L. He, X. Sun, and M.S. Dresselhaus, Appl. Phys. Lett. **72**, 3282 (1998).
[20] H. Kanzow, A. Ding, T. Belz, H. Sauer, and R. Schlögl, in *Electronic Properties of Novel Materials—Progress in Molecular Nanostructures*, edited by H. Kuzmany, J. Fink, M. Mehring, and S. Roth (AIP, New York, in press).
[21] N.M. Rodriguez, J. Mater. Res. **8**, 3233 (1993).
[22] R.S. Wagner and W.C. Ellis, Appl. Phys. Lett. **4**, 8 (1964).
[23] R.T.K. Baker, P.S. Harris, F. Henderson, and R.B. Thomas, Carbon **13**, 17 (1975).
[24] G.G. Tibbetts, J. Cryst. Growth **66**, 632 (1984).
[25] A. Oberlin, M. Endo, and T. Koyama, J. Cryst. Growth **32**, 335 (1976).
[26] A. Sacco, P. Thacker, T.N. Chang, and A.T.S. Chiang, J. Catal. **85**, 224 (1984).
[27] A.J.H.M. Kock, P.K. de Bokx, E. Boellard, W. Klop, and J.W. Geuss, J. Catal. **96**, 468 (1985).

[28] R.T.K. Baker, J.R. Alonzo, J.A. Dumesic, and D.J.C. Yates, J. Catal. **77**, 74 (1982).
[29] I. Stewart, M.J. Tricker, and J.A. Cairns, J. Catal. **94**, 360 (1985).
[30] A. Fonseca, K. Hernadi, J.B. Nagy, D. Bernaerts, and A.A. Lucas, J. Mol. Catal. A: Chem. **107**, 159 (1996).
[31] T.B. Massalski, *Binary Alloy Phase Diagrams* (ASM International, Materials Park, Ohio, 1996).
[32] K.H. Jack, Proc. R. Soc. London, Ser. A **195**, 56 (1948).
[33] M.S. Kim, N.M. Rodriguez, and R.T.K. Baker, J. Catal. **131**, 60 (1991).
[34] M. Humenik and W.D. Kingery, J. Am. Ceram. Soc. **37**, 18 (1954).
[35] W. Weisweiler and V. Mahadevan, High Temp.-High Press. **4**, 27 (1972).
[36] P. Bernier, in *Electronic Properties of Novel Materials - Progress in Molecular Nanostructures* (Ref. 20).
[37] S. Bonnamy, K. Mtnier, F. Bguin, M. Lamy de la Chapelle, S. Lefrant, C. Journet, and P. Bernier, in *Electronic Properties of Novel Materials - Progress in Molecular Nanostructures* (Ref. 20).
[38] J. Abrahamson, Carbon **11**, 337 (1973).
[39] M.V. Korobov and L.N. Sidorov, J. Chem. Thermodyn. **26**, 61 (1994).